

贵州省自然科学
优秀学术论文集

**Guizhou Collection of Excellent Academic Thesis
of Natural Science**

(2005年版)

贵州省科学技术协会

Guizhou Association For Science And Technology

贵州省自然科学优秀学术论文评审奖励委员会

主任委员：欧阳自远

副主任委员：肖伦祥

委 员：（按姓氏笔划排列）

于 杰 王明成 王国昌 朱立军

刘丛强 任湘生 伍鹏程 陈叔平

李 祥 李桂莲 周万成 周惠明

贵州省自然科学优秀学术论文理、工、 农、医、交叉学科专家评审组

理科组组长：刘丛强	副组长：俞 建
工科组组长：于 杰	副组长：杜剑平
农科组组长：李桂莲	副组长：官国倍
医科组组长：周惠明	副组长：程明亮
交叉学科组组长：任湘生	副组长：张继泽

贵州省自然科学优秀学术论文集 （2005 年版）编委会

主 编：肖伦祥

编 委：杜培术 田 雪 周 燕
刘 军 胡铁磊

责任编辑：刘 军 胡铁磊

序

2005 年，是贯彻落实科学发展观，努力实现贵州经济社会又快又好发展的关键之年，也是实施“十一五”规划的开局之年。为了贯彻落实胡锦涛总书记在全国科技大会上的重要讲话精神，动员我省广大科技工作者和社会各方面力量，共同推进我省科技事业的发展，为提高自主创新能力，建设创新型国家，实现我省经济社会发展的历史性跨越作出新贡献，贵州省科学技术协会组织开展了“移动通信杯”首届贵州省自然科学优秀学术论文的评审奖励工作。

省直有关部门，高等院校，科研院所，企业事业单位，省级学会、协会、研究会及各市、州、地科协，积极参与、支持和配合论文的筛选及推荐工作。本届评审奖励活动共收到论文 306 篇，涵盖了理、工、农、医、交叉学科五大领域，从不同行业、不同学科开展了全方位、多角度的学术研究，论文内容丰富，涉及专业众多，从不同层面反映了我省科技工作者的学术水平和研究成果，为最终评选出我省高质量、高水平的优秀学术论文奠定了坚实的基础。

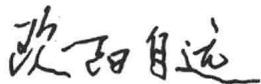
贵州省科协为保证本届评审奖励活动的顺利有序进行，专门成立了贵州省自然科学优秀学术论文评审奖励委员会及贵州省自然科学优秀学术论文理、工、农、医、交叉学科专家评审组，选聘我省各学科领域的多位知名专家对论文进行认真评审。在严格掌握标准，宁缺毋滥的原则下，使评审奖励工作做到了“公平、公开、公正”。经专家认真工作，达到了预期目标，遴选出了优秀学术论文一等奖 5 篇，二等奖 20 篇，三等奖 40 篇，提名奖 11 篇，较好地体现了我省这一时期的学术研究水平。

“移动通信杯”首届贵州省自然科学优秀学术论文的评审奖励工作在全社会产生了较大、较好的影响，为广大科技工作者做了一件实事、好事，搭建了学术交流和服务广大科技工作者的平台。开展贵州省自然科学优秀学术论文评审奖励活动，对促进全省学术繁荣、学科发展、人才成长和科技进步，全面实施人才强省战略，建立完善科协的表彰激励机制，充分调动广大科技工作者的积极性和创造性，为省的经济建设和社会发展起到了积极的推动作用。

这次评审奖励活动得到贵州省及贵阳市移动通信公司的鼎力支持，并冠名“移动通信杯”，为评审工作的圆满成功提供了有力保障。这是建立和完善科技评审奖励机制的有益尝试，引起了社会各界的高度关注，吸引了省内企业的积极参与，为科协的改革和发展进行了一次较为成功的探索。

“移动通信杯”首届贵州省自然科学优秀学术评审奖励活动取得圆满成功，是与社会各界的大力支持和积极参与分不开的。值此《贵州省自然科学优秀学术论文集（2005 年版）》付梓之际，谨向获奖的论文作者表示热烈的祝贺！向积极参与评审奖励活动并付出辛勤劳动的专家、工作人员及有关单位表示诚挚的谢忱！

贵州省科协主席
中国科学院院士



二 00 六年二月

目 录

一等奖

Faddeev-Jackiw 方法对非对易性研究·····	隆正文, 荆坚 (1)
琵琶湖水体不同分子量溶解有机质组分中分子荧光和氨基酸特征研究·····	吴丰昌, 田上英一郎, 刘从强 (5)
水稻 micro RNA 的分离、克隆及鉴定·····	王嘉福, 周惠, 陈月琴, 罗庆军, 屈良鹄 (15)
虫生菌物 <i>Cordyceps jiangxiensis</i> 菌体及多糖的深层培养条件优化·····	肖建辉, 陈代雄, 刘金伟 (25)
数字影像会诊系统的创建及初步应用·····	王学建, 胡建, 曹军, 王波, 焦俊, 魏渝清, 王小林, 罗敏, 罗松 (39)

二等奖

$P_n(\Gamma)$ 一组 Hilbert 基的判定和计算·····	岑燕明 (44)
一种来自于额外维空间的新能源·····	陶必修, 吉世印, 李芳琼 (51)
贵州寒武系的楔叶虫: 一种底栖固着的食肉动物·····	彭进, Loren E Babcock, 赵元龙, 王平丽, 杨荣军 (58)
铁路振动及其在岩溶塌陷中的致塌力研究·····	程星, 黄润秋 (67)
中国天山冰芯记录中人类对偏远地区大气的污染·····	李心清, 秦大河, 江桂斌, 段克勤, 周会 (72)
各种大跨度拟梁式桁架结构的特性与技术经济指标·····	马克俭, 郑涛, 张华刚, 丁婷, 郭明明, 周观根 (87)
钛合金表面宽带激光熔覆梯度生物陶瓷复合涂层的动力学研究·····	刘其斌, 邹龙江, 朱维东, 李海涛, 董闯 (100)
自然界中 ZnS-CdS 完全类质同象系列的发现和初步研究·····	刘铁庚, 张乾, 叶霖, 邵树勋 (107)
三轴应力条件下红粘土力学特性动态变化的 CT 分析·····	黄质宏, 朱立军, 蒲毅彬, 周训华 (112)
黔东南州气象灾害对水稻生产影响的研究及对策·····	池再香, 白慧, 罗顺楨, 石宏辉 (117)
造林技术措施对马尾松林分生长影响的定量分析与预测·····	温佐吾 (121)
玉米 O2 基因内三个微卫星位点的隐性等位变异·····	杨文鹏, 郑用琰, 倪深, 吴菁 (126)
两种淡水鱼——草鱼和胡子鲇的肥大细胞·····	许乐仁, 杨筱珍, 高登慧, 江萍 (137)
采用十二指肠镜及腹腔镜联合治疗重症胆管炎·····	张翔, 秦建国, 庞家芳, 韩民, 苟欣, 黄晓锋 (143)
皮瓣重建阴囊及其对精子发生的影响·····	王达利, 郑洪, 邓飞 (145)
银杏叶提取物对正常大鼠海马 caspase-3 和淀粉样前体蛋白水平的影响·····	罗璨, 吴芹, 黄燮南, 孙安盛, 石京山 (151)
脑卒中患者血管紧张素转换酶基因多态性与心率变异性的关联研究·····	王艺明, 刘兴德, 董为伟, 杨宗城 (157)
制约逻辑是内涵智能机的逻辑理论基础·····	龚启荣, 林邦瑾 (162)
电力市场环境发电公司风险管理框架·····	刘敏, 吴复立 (166)
基于生产要素时空——动态价值量优势的企业“走出去”战略·····	陈泽明 (172)

三等奖

- 中国蚰属蚰亚属盾纹组分类纪要并三新种记述（双翅目，蚰科）·····陈汉彬（193）
- 中国凹距飞虱族（半翅目：蜡蝉总科：飞虱科）分属检索表及一新属记述·····陈祥盛（199）
- Gauss-Markov 条件下最小二乘估计的强相合性·····金明仲，吴贤毅，金良琼（206）
- 全连续算子谱逼近的后验误差估计·····杨一都，黄秋梅（213）
- 新型含氟 α -氨基膦酸酯的合成和晶体结构·····杨松，宋宝安，吴扬兰，金林红，刘刚，胡德禹，卢平（220）
- 用量子受限模型分析硅氧化层中的锗低维纳米结构·····黄伟其，刘世荣（224）
- 贵州四个洞穴滴水对大气降雨响应的动力学及意义·····周运超，王世杰，谢兴能，罗维均，黎廷宇（229）
- 鲤科鲃亚科鲃群鱼类的系统发育及动物地理学·····代应贵，杨君兴（237）
- 论碳酸盐岩现代风化壳和古风化壳·····李景阳，朱立军（259）
- 浅论利用波速测试成果综合选取坝基岩体承载力问题·····余波，徐光祥（265）
- 铝基型芯脱芯剂的研究及在航空发动机叶片制造中的应用·····李林，刘建平（271）
- GDL-1 型汽车齿轮的微变形、高强韧性材料及热加工工艺的研究与应用·····梁益龙，雷旻，陈伦军，张晓燕，高宏（272）
- 四角切圆燃烧技术（300MW 机组）首次燃用贵州低挥发份无烟煤的经验·····张建兴（277）
- 岩溶地区设计洪水计算的探讨·····杨全明，尹明万，李景海（294）
- 斜轴式液压泵压力跳动的故障分析与排除·····梁贵萍（299）
- SPOT5 在矿山监测中的应用·····况顺达，赵震海（303）
- PB7.0 通用任意字段查询技术的实现·····张梅（308）
- 高抗冲聚苯乙烯的应变率敏感性及其粘塑性本构关系·····蔡长安，于杰，罗筑，刘一春（312）
- 贵州喀斯特山地坡耕地立地影响因素及分区·····张喜（318）
- 应用细胞自动机(CA)模型研究植物种群在可控制系统中的扩散机制：一年生杂草作为一个应用实例·····
·····王季槐，M. J. Kropff, B., Lammert, S., Christensen, P. K. Hansen（323）
- 小菜蛾对溴氰菊酯的抗性消退与抗性恢复动态·····李凤良，李忠英，韩招久，陈之浩（333）
- 黄壤坡地土壤水分入渗垂直变异特征分析·····蒋太明，肖厚军，刘海隆，刘洪斌（337）
- 大粒组荞麦种的细胞学、同工酶及种间杂交研究·····陈庆富，Sai. L. K. Hsam, Friedrich J. Zeller（343）
- 利用形态学、RAPD 及 AFLP 标记鉴定刺梨及其近缘种的遗传关系·····文晓鹏，庞晓明，邓秀新（347）
- 用同位素 ^{15}N 直接法和间接法研究小麦/蚕豆间作中根系相互作用对种间竞争及氮转移的影响·····肖焱波，李隆，张福锁（357）
- 建设生态畜牧业大省的内涵及路径探讨·····彭志良，王天生（364）
- 626 例少数民族育龄妇女避孕现状分析·····许吟，李裕，鲍优兰（368）
- 头针及推拿治疗腰椎间盘突出症及其对自身免疫水平的影响·····崔瑾，向开维，梁永瑛（370）
- 热休克蛋白 70-肿瘤肽的纯化及其抗小鼠肝癌免疫效应·····陈代雄，苏艳蓉，邵根泽（374）
- 白细胞介素 17 在大鼠慢性阻塞性肺疾病和支气管哮喘模型中的变化及意义·····
·····沈锋，赵鸣武，贺蓓，杨京京，裴裴，王玉柱（382）

1439 例眼外伤病例的临床分析·····	金鸣昌, 潘海燕, 陶娅, 代丽伟, 欧阳光明 (387)
补充 NaFe-EDTA 对学龄儿童青少年贫血及血清铁蛋白水平的影响研究·····	汪思顺, 卢启良, 王素芳, 赵显峰 (389)
钩藤碱对脑缺血/再灌损伤的保护作用·····	吴二兵, 孙安盛, 吴芹, 余丽梅, 石京山, 黄燮南 (392)
中药泻火养阴散治疗初发弥漫性甲状腺肿大并甲亢 30 例临床观察·····	李雪梅, 曹永芬, 杨娟, 郭茜 (395)
左-卡尼汀对体外循环心瓣膜替换术患者心肌的保护作用·····	向道康, 阎兴治, 杨世虞, 刘秀伦, 胡选义, 周涛 (398)
弓形虫速殖子表膜蛋白的组分和抗原性分析·····	王世海, 熊美华, 唐丽娜, 王秀珍, 刘露霞 (402)
高校创办科技教育专业及青少年科技教育实践基地的研究·····	钱贵晴, 任钢建, 谷丽应, 董旭, 徐文祥, 陈爽, 李松 (405)
我国银行业市场竞争结构的实证分析——基于 Panzar-Rosse 范式的考察·····	赵子铤, 彭琦, 邹康 (409)
中国人口预测的自回归分布滞后模型研究·····	安和平 (415)
基于 Web 制造执行系统的实现技术·····	景亚萍 (423)

提名奖

两种鼠蚤在新羽化和吸血后不同时间三种酶的组织化学研究·····	寻慧, 漆一鸣 (427)
GIS 技术在划分巴西陆稻“IAPAR9”适宜种植区域中的应用·····	郑小波, 康为民, 汪圣洪, 吴俊铭 (432)
^{124}Te 核 1^+ 态和高自旋态能谱特征的微观研究·····	石筑一, 倪绍勇, 童红, 赵行知 (436)
青藏铁路昆仑山口高含冰量冻土路堑换填保温施工技术·····	王永义 (439)
贵州喀斯特地区洪涝灾害特征及减灾对策·····	王继辉, 杨明, 顾小林, 杨玲, 彭桂玉 (445)
贵州省毕节地区畜禽寄生虫的区系调查与防治效益·····	阮正祥, 王勤, 曾志明, 杨阿莎, 何虎, 苟中屏, 杨廷军, 杨福芬, 邱声邦, 郝琼, 江凤霞, 朱武清 (449)
美国水稻品种对稻瘟病小种 IE-1k、IB-33、IB-49 和 IC-17 的抗性遗传·····	严宗卜 (452)
生态农业“三维”复合系统的运行机制与运作方式·····	王秀峰, 伍国勇 (458)
瘦素、细胞因子及胰岛素抵抗与心功能不全关系的研究·····	汪晓云, 廖昆灵, 卢微, 陈雪英, 刘路 (467)
贵州苗药大果木姜子研究及产业化·····	邱德文, 杜茂端 (470)
燃煤型砷中毒患者遗传损伤及癌变机理·····	张爱华, 洪峰, 黄晓欣, 罗鹏, 胡昌军, 刘忠义, 杨光红 (475)

Faddeev - Jackiw approach to the noncommutativity

Zheng-Wen Long¹, Jian Jing²

1. Department of Physics, GuiZhou University, GuiYang 550025, PR China

2. Theoretical Physics Division, Nankai Institute of Mathematics, Nankai University, Tianjin 300071, PR China

Abstract: We apply the Faddeev - Jackiw (FJ) method to the open string in the D-brane background with a nonvanishing B-field. The reduced phase space was obtained directly by solving the mixed boundary conditions. The noncommutativity of coordinates along the D-brane was reproduced. Some ambiguities in the previous papers could be avoided by this method.

Keywords: Faddeev - Jackiw method; String theory; Noncommutativity; Boundary conditions

Faddeev-Jackiw 方法对非对易性研究

隆正文¹, 荆坚²

(1. 贵州大学物理系, 贵州 贵阳 550025;

2. 南开大学数学学院理论物理学处, 天津 300071)

对非对易空间的研究, 最早可追溯到上世纪四十年代, 杨振宁和 H. S. Snyder 等人的工作, 那时认为由于引力的存在, 时空坐标之间有可能是非对易的, 在某些特定的情况下, 这种对时空代数的修改会对量子场论的紫外发散行为有所改散, 最近这个问题再一次成为理论物理研究的热点问题之一则是由超弦理论的研究引发的, 超弦理论的研究表明, D 膜的有效低能理论在 NS-NSB 背景场下, 其世界体方向坐标之间满足非对易关系, 超弦理论的唯一象学猜测, 我们所生存的现实空间有可能就是一个 D 膜的世界体, 这一点被越来越多的理论物理学家所认同, 因此, 我们所生存的现实空间有可能就是非对易空间。

我们研究了当存在 NS-NSB 背景场时开弦的端点在 D 膜上的非对易性质, 这个问题是在弦理论中的研究中提出来的, 并且由此掀起了关于非对易几何在理论物理中的研究热潮, 以前对 D 膜表面的非对易的导出, 都是用 Dirac 方法, 将边界条件作为 Dirac 约束来处理, 然而这种初级约束和传统的 Dirac 约束有不同的起源, 传统的 Dirac 约束是由于奇异拉氏量引起的, 将边界条件当作 Dirac 约束来处理会带来取不同的弱收敛形式得到不同的结果以及理论的真实自由度为负无穷等一系列的问题。

我们首次应用 Faddeev-Jackiw 方法对这个问题进行了深入的分析, 与先前的大多数文献不同的是, 我们对弦空间进行了离散化处理, 就避免了有关 δ 函数的问题, 通过直接求解边界条件得到约化的相空间, 这样就成功地避免了关于处理约束条件的问题, 最后我们通过辛矩阵的计算, 直接从他的逆矩阵中读出了对易关系, 避免了对 δ 函数的正规化处理问题, 通过计算我们得到了只有在端点非对易的, 这和目前人们普遍接受的观点是一致的, 纠正了 M. M. Sheikh, Jabbari 等人用 Dirac 方法作出的在端点和端点附近都是非对易的错误。

Noncommutativity has attracted much attention in the past a few years^[1]. It is widely believed that the open strings attached to D-branes in the presence of background B-field would induce noncommutativity in its end points^[2-4]. The most conventional way to derive this noncommutativity is to use Dirac brackets^[5], which were proposed by Dirac more than half a century, and treat the mixed boundary conditions (BCs) as primary constraints. However, recently there are some renewed interests on this subject^[6,7], and some discrepancies appears.

One of the focuses of these ambiguities is how to treat the mixed BCs. In Refs.^[2,4,8], these BCs were treated as primary Dirac constraints, subsequently, an infinite set of secondary second class constraints could be obtained by the consistent requirements. It is quite amazing that such circumstances rarely happened before. In a more recent paper^[6], the author announced that if the BCs were treated as primary constraints, then the Dirac method would not lead to an infinite set of secondary constraint chains but to a finite one, also, the noncommutative algebras would not appear. So it is necessary to study this problem from another point of view.

The purpose of the present Letter is to analyze this problem in an alternative way, that is, we shall apply

FJ method^[9] to this problem. The advantage of this method is that we need not classify the constraints into the so-called primary or secondary, the first class or the second class, so the ambiguities mentioned above could be avoided. We shall work in the discrete version, find the reduced phase directly by solving the mixed BCs, and then read the commutators directly.

The action for an open string with its end points attaching on a D-brane in the presence of NS B-field is (our convention are almost the same as^[4])

$$S = \frac{1}{4\pi\alpha'} \int d^2\sigma \left[g^{\alpha\beta} \eta_{\mu\nu} \partial_\alpha X^\mu \partial_\beta X^\nu + 2\pi\alpha' B_{\mu\nu} \epsilon^{\alpha\beta} \partial_\alpha X^\mu \partial_\beta X^\nu \right] + \int d\tau A_\mu \partial_\tau X^\mu \Big|_{\sigma=\pi} - \int d\tau A_\mu \partial_\tau X^\mu \Big|_{\sigma=0}, \quad (1)$$

where $g_{\alpha\beta} = \text{diag}(-, +)$, $\epsilon^{01} = -\epsilon^{10} = 1$, $B_{\mu\nu} = -B_{\nu\mu}$, $\eta_{\mu\nu} = \text{diag}(-, +, \dots, +)$, and the length of string is π . In the case of both the end points attaching on the same D-brane, the last two terms can be written as

$$-\frac{1}{2\pi\alpha'} \int d^2\sigma F_{\mu\nu} \epsilon^{\alpha\beta} \partial_\alpha X^\mu \partial_\beta X^\nu$$

and the action (1) is

$$S = \frac{1}{4\pi\alpha'} \int d^2\sigma \left[g^{\alpha\beta} \eta_{\mu\nu} \partial_\alpha X^\mu \partial_\beta X^\nu + 2\pi\alpha' \mathcal{F}_{\mu\nu} \epsilon^{\alpha\beta} \partial_\alpha X^\mu \partial_\beta X^\nu \right], \quad (2)$$

where $\mathcal{F} = B - F = B - dA$, which is invariant under both $U(1)$ gauge transformation, $A \rightarrow A + d\lambda$, and the so-called Λ translation, $A \rightarrow A + \Lambda$, $B \rightarrow B + d\Lambda$. Without loss of any generality, we put the electric mixing, i.e., $\mathcal{F}_{0\mu} = \mathcal{F}_{\mu 0} = 0$ [4], and for the sake of simplicity, we set $2\pi\alpha' = 1$ and recover it when it is necessary.

The variation of (2) gives both the equation of motion and the mixed BCs, respectively,

$$(\partial_\tau^2 - \partial_\sigma^2) X^\mu = 0, \quad (3)$$

$$(\partial_\sigma X^\mu - \mathcal{F}^\mu{}_\nu \partial_\tau X^\nu)_{\sigma=0,\pi} = 0. \quad (4)$$

In Refs.^[2,4,8], the above BCs are treated as primary constraints, and the Dirac's methods were used to derive the noncommutative algebras. Because these BCs are only valid on the D-brane's world volume, so some singularities just as $\delta(\sigma)$ or $\delta(\sigma - \pi)$ (or even the derivatives of these terms) must be introduced^[3]. It is also a tedious task to find all the constraints and then calculate the Dirac brackets. In order to avoid such singularities and the calculation of Dirac brackets, we shall work in the discrete version, which means that we discretize σ , and denote the steps by $\varepsilon = \pi/N$, so that the continuum theory can be obtained by taking the limit $\varepsilon \rightarrow 0$ or $N \rightarrow \infty$.

The action and the BCs in the discrete version are

$$S = \frac{1}{4\pi\alpha'} \int dt \left[- \sum_{i=0}^N \varepsilon \eta_{\mu\nu} \dot{X}_i^\mu \dot{X}_i^\nu + \sum_{i=0}^{N-1} \frac{1}{\varepsilon} \eta_{\mu\nu} (X_{i+1} - X_i)^\mu (X_{i+1} - X_i)^\nu + 2\mathcal{F}_{\mu\nu} \sum_{i=0}^{N-1} \dot{X}_i^\mu (X_{i+1} - X_i)^\nu \right], \quad (5)$$

$$\frac{1}{\varepsilon} (X_1 - X_0)^\mu - \mathcal{F}^\mu{}_\nu \partial_\tau X_0^\nu = 0, \quad (6)$$

$$\frac{1}{\varepsilon} (X_\pi - X_{\pi-\varepsilon})^\mu - \mathcal{F}^\mu{}_\nu \partial_\tau X_\pi^\nu = 0, \quad (7)$$

and the equations of motion in this discrete form are

$$\varepsilon \partial_t^2 X_0^\mu = \frac{1}{\varepsilon} (X_1 - X_0)^\mu, \quad (8)$$

$$\varepsilon \partial_t^2 X_i^\mu = \frac{1}{\varepsilon} (X_{i+1} - 2X_i + X_{i-1})^\mu, \quad i \neq 0, N, \quad (9)$$

$$\varepsilon \partial_t^2 X_\pi^\mu = \frac{1}{\varepsilon} (X_\pi - X_{\pi-\varepsilon})^\mu. \quad (10)$$

From the above discrete version of BCs, we see that it is sufficient for us only to take two points, say, X_0^μ, X_1^μ (for the other end, the analysis is almost the same, we only give our results) into consideration.

The action for these two points in the discrete form are

$$S = \frac{1}{4\pi\alpha'} \int dt \left[-\eta_{\mu\nu} \epsilon \dot{X}_0^\mu \dot{X}_0^\nu - \eta_{\mu\nu} \epsilon \dot{X}_1^\mu \dot{X}_1^\nu + \frac{1}{\epsilon} \eta_{\mu\nu} (X_1 - X_0)^\mu (X_1 - X_0)^\nu \right. \\ \left. + \frac{1}{\epsilon} \eta_{\mu\nu} (X_2 - X_1)^\mu (X_2 - X_1)^\nu + 2\mathcal{F}_{\mu\nu} \dot{X}_0^\mu (X_1 - X_0)^\nu + 2\mathcal{F}_{\mu\nu} \dot{X}_1^\mu (X_2 - X_1)^\nu \right]. \quad (11)$$

Now there are two methods to proceed on. One is the traditional Dirac method. It takes the BCs(6) (or(7)) as the Hamiltonian primary constraints^[4,8] in which the Lagrange multipliers are introduced in order to construct the so-called total Hamiltonian and then exhaust all the constraint chains or determine the Lagrangian multipliers by the consistent requirements, finally the commutation relations can be obtained by calculating Dirac brackets. However, a new feature beyond the ordinary Dirac context would appear if we treat the BCs as the Dirac primary constraints^[4,8], that is the Lagrange multipliers are determined by the consistent requirement while the constraints chains are not terminated. It is quite amazing that such situations rarely happened before. In a recent paper^[6], the author finds that in the Dirac context, if the BCs are treated as the primary constraints, then the constraint chains are not infinite but finite, and the noncommutative algebras will not appear, furthermore, the author stress that the noncommutative algebras will not appear even if one insist that the constraint chains are infinite. So in this Letter we shall analyze this problem by using the Faddeev - Jackiw method.

According to FJ^[9], we shall find the reduced phase space and re-express the action(11) in a first-order form in this reduced phase space. In doing so, we solve the BCs(6) and substitute the BCs(6) into the Lagrangian(11), the reduced phase space is obtained and the action which is related with the X_μ^0 is written as the first-order form

$$S = \frac{1}{2} \int dt [(\mathcal{F}^{-1}M)_{\mu\nu} (X_1 - X_0)^\mu \dot{X}_0^\nu + \mathcal{L}_{X_1}], \quad (12)$$

where $M = 1 - \mathcal{F}^2$, and

$$\mathcal{L}_{X_1} = -\eta_{\mu\nu} \epsilon \dot{X}_1^\mu \dot{X}_1^\nu + 2\mathcal{F}_{\mu\nu} \dot{X}_1^\mu (X_2 - X_1)^\nu + \frac{1}{\epsilon} \eta_{\mu\nu} (X_2 - X_1)^\mu (X_2 - X_1)^\nu. \quad (13)$$

Because the BCs (6) are not complicated, it is easy to find the reduced phase space directly by solving BCs (6), and we are allowed to work in this reduced phase space, so the introduction of the conjugate momenta ($P_{0\mu}$) to the point X_0^μ is not needed.

As there are no constraints on the variables $X_{1\mu}$, the Lagrangian \mathcal{L}_{X_1} is treated in the standard way, that is, we introduce the conjugate momenta $P_{1\mu}$ to X_μ . It is defined as usual,

$$P_{1\mu} = \frac{\delta S}{\delta \dot{X}_1^\mu} = \mathcal{F}_{\mu\nu} (X_2 - X_1)^\nu - \epsilon \dot{X}_{1\mu}, \quad (14)$$

and the Hamiltonian corresponding to \mathcal{L}_{X_1} is

$$\mathcal{H}_{X_1} = P_{1\mu} \dot{X}_1^\mu - \mathcal{L}_{X_1} \\ = -\frac{1}{2\epsilon} P_{1\mu} P_1^\mu - \frac{1}{2\epsilon} M_{\mu\nu} (X_2 - X_1)^\mu (X_2 - X_1)^\nu + \frac{1}{\epsilon} P_1^\mu \mathcal{F}_{\mu\nu} (X_2 - X_1)^\nu. \quad (15)$$

Hence, the Lagrangian \mathcal{L}_{X_1} is written in the first-order form as

$$\mathcal{L}_{X_1} = P_{1\mu} \dot{X}_1^\mu - \mathcal{H}_{X_1}, \quad (16)$$

where the Hamiltonian \mathcal{H}_{X_1} had been given in (15).

We have 'translated' the action (11) into the first-order form,

$$S = \int dt \left\{ \frac{1}{2} (\mathcal{F}^{-1}M)_{\mu\nu} (X_1 - X_0)^\mu \dot{X}_0^\nu + P_{1\mu} \dot{X}_1^\mu - \mathcal{H}_{X_1} \right\}. \quad (17)$$

A set of symplectic variables, $\xi_i^\mu = (X_0^\mu, X_1^\mu, P_1^\mu)$, and the corresponding canonical one-form

$$a_{i\mu} = \left(\frac{1}{2} (\mathcal{F}^{-1}M)_{\nu\mu} (X_1 - X_0)^\nu, P_{1\mu}, 0 \right)$$

can be read from action (17). These result in the symplectic two-form matrix f

$$(f_{\mu\nu})_{ij} = \frac{\partial(a_\nu)_j}{\partial(\xi^\mu)^i} - \frac{\partial(a_\mu)_i}{\partial(\xi^\nu)^j}. \quad (18)$$

According to the FJ, if the matrix f is regular, then the commutators can be read from the inverse of it directly. To show how the FJ method works, for the sake of simplicity and without loss of generality, we restrict ourselves to the D2-brane^[4], in this case $\mu, \nu=1,2$ and the f is a 6×6 matrix. After some simple calculations, we give the explicit expression of the matrix below,

$$f = \begin{pmatrix} 0 & -\frac{1}{2\pi\alpha'}(\mathcal{F}^{-1}M)_{12} & 0 & \frac{1}{4\pi\alpha'}(\mathcal{F}^{-1}M)_{12} & 0 & 0 \\ \frac{1}{2\pi\alpha'}(\mathcal{F}^{-1}M)_{12} & 0 & -\frac{1}{4\pi\alpha'}(\mathcal{F}^{-1}M)_{12} & 0 & 0 & 0 \\ 0 & \frac{1}{4\pi\alpha'}(\mathcal{F}^{-1}M)_{12} & 0 & 0 & -1 & 0 \\ -\frac{1}{4\pi\alpha'}(\mathcal{F}^{-1}M)_{12} & 0 & 0 & 0 & 0 & -1 \\ 0 & 0 & 1 & 0 & 0 & 0 \\ 0 & 0 & 0 & 1 & 0 & 0 \end{pmatrix}. \quad (19)$$

Here we recover the coefficient $2\pi\alpha'$ explicitly. Obviously, f is not singular provided $\mathcal{F}_{\mu\nu}$ no vanishing, hence the inverse of this matrix exists,

$$f^{-1} = \begin{pmatrix} 0 & 2\pi\alpha'(M^{-1}\mathcal{F})_{12} & 0 & 0 & \frac{1}{2} & 0 \\ -2\pi\alpha'(M^{-1}\mathcal{F})_{12} & 0 & 0 & 0 & 0 & \frac{1}{2} \\ 0 & 0 & 0 & 0 & 1 & 0 \\ 0 & 0 & 0 & 0 & 0 & 1 \\ -\frac{1}{2} & 0 & -1 & 0 & 0 & \frac{1}{8\pi\alpha'}(M^{-1}\mathcal{F})_{12} \\ 0 & -\frac{1}{2} & 0 & -1 & -\frac{1}{8\pi\alpha'}(M^{-1}\mathcal{F})_{12} & 0 \end{pmatrix}. \quad (20)$$

From the above matrix f^{-1} , we can read the following commutators,

$$\begin{aligned} \{X_0^\mu, X_0^\nu\} &= 2\pi\alpha'(M^{-1}\mathcal{F})^{\mu\nu}, & \{X_0^\mu, X_1^\nu\} &= 0, & \{X_1^\mu, X_1^\nu\} &= 0, \\ \{X_0^\mu, P_{1\nu}\} &= \frac{1}{2}\delta_\nu^\mu, & \{X_1^\mu, P_{1\nu}\} &= \delta_\nu^\mu. \end{aligned} \quad (21)$$

For the other end, the action in the discrete form are

$$\begin{aligned} S = \frac{1}{4\pi\alpha'} \int dt & \left[-\eta_{\mu\nu}\varepsilon\dot{X}_\pi^\mu\dot{X}_\pi^\nu - \eta_{\mu\nu}\varepsilon\dot{X}_{\pi-\varepsilon}^\mu\dot{X}_{\pi-\varepsilon}^\nu + \frac{1}{\varepsilon}\eta_{\mu\nu}(X_\pi - X_{\pi-\varepsilon})^\mu(X_\pi - X_{\pi-\varepsilon})^\nu \right. \\ & + \frac{1}{\varepsilon}\eta_{\mu\nu}(X_{\pi-\varepsilon}^\mu - X_{\pi-2\varepsilon}^\mu)(X_{\pi-\varepsilon}^\nu - X_{\pi-2\varepsilon}^\nu) + 2\mathcal{F}_{\mu\nu}\dot{X}_\pi^\mu(X_\pi - X_{\pi-\varepsilon})^\nu \\ & \left. + 2\mathcal{F}_{\mu\nu}\dot{X}_{\pi-\varepsilon}^\mu(X_{\pi-\varepsilon} - X_{\pi-2\varepsilon})^\nu \right]. \end{aligned} \quad (22)$$

The boundary conditions and the equation of motion have been given in(7), (10), the analysis can be done in the same manner, and the final results are

$$\begin{aligned} \{X_\pi^\mu, X_\pi^\nu\} &= -2\pi\alpha'(M^{-1}\mathcal{F})^{\mu\nu}, & \{X_\pi^\mu, X_{\pi-\varepsilon}^\nu\} &= 0, & \{X_{\pi-\varepsilon}^\mu, X_{\pi-\varepsilon}^\nu\} &= 0, \\ \{X_\pi^\mu, P_{(\pi-\varepsilon)\nu}\} &= \frac{1}{2}\delta_\nu^\mu, & \{X_{\pi-\varepsilon}^\mu, P_{(\pi-\varepsilon)\nu}\} &= \delta_\nu^\mu. \end{aligned} \quad (23)$$

Our results mainly agree with that of^[4,8], except a little difference, there, not only the end points, but also the points which are neighbouring to the end points (i.e., X_1^μ or $X_{\pi-\varepsilon}^\mu$) are also noncommutative.

Acknowledgement

This work is supported by the National Natural Science Foundation of China with grant No. 10247009.

References

- [1] N. Seiberg, E. Witten, JHEP 99009 (1999) 032, hep-th/9908142.
- [2] C. S. Chu, P. M. Ho, Nucl. Phys. B 550 (1999) 151, hep-th/9812219.
- [3] C. S. Chu, P. M. Ho, Nucl. Phys. B 568 (2000) 447, hep-th/9906192.
- [4] F. Ardalan, H. Arfaei, M. M. Sheikh-Jabbari, Nucl. Phys. B 576 (2000) 578, hep-th/9906161.
- [5] P. A. M. Dirac, Lecture Notes on Quantum Mechanics, Yeshiva University, New York, NY, 1964.
- [6] F. Loran, Phys. Lett. B 544 (2002) 199.
- [7] W. He, L. Zhao, Phys. Lett. B 532 (2002) 345, hep-th/0111041.
- [8] M. M. Sheikh-Jabbari, A. Shirzad, Eur. Phys. J. C 19 (2001) 383.
- [9] L. D. Faddeev, R. Jackiw, Phys. Rev. Lett. 60 (1988) 1691.

Fluorescence and amino acid characteristics of molecular size fractions of DOM in the waters of Lake Biwa

F. C. WU^{1,3}, E. TANOUE² and C. Q. LIU¹

¹The State Key Laboratory of Environmental Geochemistry, Institute of Geochemistry, Chinese Academy of Sciences, Guiyang/Guizhou, 550002, China; ²Department of Earth and Environmental Sciences, Graduate School of Environmental Studies, Nagoya University, Nagoya, 464-8601, Japan; ³Current address: Environmental and Resource Studies, Trent University, 1600 West Bank Drive, Peterborough, K9J 7B8, Ontario, Canada

Abstract. Dissolved organic matter (DOM) in the waters from Lake Biwa, Japan was fractionated using tangential flow ultrafiltration, and subsequently characterized by fluorescence properties and amino acids. While major dissolved organic carbon (DOC), UV absorbance (Abs), humic-like fluorescence (Flu) and total hydrolyzed amino acids (THAA) occurred in the less than 5 kDa molecular size fraction, they were not evenly distributed among various molecular size fractions. Flu/Abs ratios increased, and THAA/DOC ratios decreased with decreasing molecular size. Humic-like fluorescence occurred in all molecular size fractions, but protein-like fluorescence only occurred in the 0.1 μm -GF/F fraction. Subtle differences in amino acid compositions (both individuals and functional groups) were observed between various molecular size fractions, this may indicate the occurrence of DOM degradation from higher to lower molecular weight. The results reported here have significance for further understanding the sources and nature of DOM in aquatic environments.

Key words: Amino acids; Degradation; Dissolved organic matter; Fluorescence; Fractionation

琵琶湖水体不同分子量溶解有机质组分中分子 荧光和氨基酸特征研究

吴丰昌¹, 田上英一郎², 刘丛强¹

(1. 中国科学院地球化学研究所环境地球化学国家重点实验室;

2. 日本名古屋大学环境科学研究生院地球与环境科学系)

溶解有机质在水生态系统中具极其重要的功能, 它不仅是物质能量和营养组分循环的重要途径、而且控制着有毒污染物的化学形态、毒性和生物吸收。因此, 一直是国际环境科学领域的热点之一, 是当前水环境污染控制和生态修复技术中关键的基础理论和科学问题。本文运用测向超滤将水体中溶解有机质分离成不同分子量组分, 详细研究了不同组分的分子荧光、氨基酸组成特征和循环规律, 系统地揭示了溶解有机质中分子量分布、物理结构和化学组成之间的内在关系。该研究对认识溶解有机质的生物地球化学循环、生态环境效应和功能具有重要意义。

结果表明: 溶解有机碳、紫外吸收、腐殖质荧光和总水解氨基酸主要分布在小于 5 千道尔顿 (Da) 分子量的有机组分中。但是, 它们在不同分子量有机组分中的分布是不均匀的。随着分子量的减小, 其组分的荧光与紫外吸收的比值, 及总氨基酸与总有机碳的比值都增大。腐殖质荧光分布在所有不同分子量组分中, 而类蛋白荧光只分布在大分子量组分中。同时该论文还发现了不同分子量有机组分中氨基酸化学组成 (单个组成和功能团特征) 存在着显著差别, 暗示存在分子量从大到小的溶解有机质降解过程, 及来源差异性。结果对进一步认识水环境中溶解有机质的源和本质有十分重要的意义。

目前, 我们对有关溶解有机质中物理化学特征和分子量大小之间关系的认识还很少。该论文为认识荧光和氨基酸组成之间关系的研究提供了一些新的线索。结果表明, 0.1 μm -GF/F 分子量有机组分含有相对高含量的氨基酸, 特别含有相对高含量的酸性和芳香族类型氨基酸。不同分子量大小有机组分之间氨基酸相对组成的差别明显。所有有机组分含有类似的腐殖质荧光特征, 但特殊的类蛋白荧光特征只存在于 0.1 μm -GF/F 分子量的有机组分中。因此, 0.1 μm -GF/F 分子量有机组

分很有可能是现代生物来源, 代表了新近产生的有机物质, 而较低分子量的有机组分则经历了较大程度的降解作用。

Introduction

In aquatic environments, molecular mass distribution and characteristics of DOM have been reported in terms of elemental (C, N) and isotopic (^{13}C and ^{14}C) composition, fluorescence and absorbance (Smith 1976; Stewart and Wetzel 1980; Carlson et al. 1985; Hart et al. 1992; Guo et al. 1994; Martin et al. 1995; Guo and Santschi 1996; Mopper et al. 1996; Guo and Santschi 1997). These studies showed that although major DOC was mainly in the less than 5 kDa molecular size fractions, and minor DOC in the $>0.1\ \mu\text{m}$ fractions, the chromophoric properties and chemical compositions of DOM were not evenly distributed among different molecular size fractions. Recent studies on metal binding characterization (Salbu et al. 1987; Orlandini et al. 1990; Hart et al. 1992; Guo et al. 1994; Martin et al. 1995; Wu et al. 2001; Wu and Tanoue 2001a) also indicated that there did exist evident differences in the properties and nature of DOM in different molecular size fractions.

Recently, three dimensional excitation/emission (Ex/Em) matrix spectroscopy (3DEEM) has been used successfully to probe the chemical structure of DOM due to its ability to distinguish different classes of organic matter (Coble et al. 1990; Senesi 1990; Mopper and Schultz 1993; Del Castillo et al. 1999; Mayer et al. 1999). HPLC has been also used to detect amino acid compositions in studies of DOM biogeochemical cycling in aquatic environments (Robertson et al. 1987; Berdie et al. 1995; Colombo et al. 1998; Wu and Tanoue 2001b). These methods, however, have never been used to investigate various molecular size fractions of DOM.

In this paper, an initial investigation was carried out to explore fluorescence and amino acid characteristics, and the possible interrelationship of various molecular size fractions of DOM. 3DEEM and HPLC, coupled with both acid and alkaline hydrolysis, were used. Tangential flow ultrafiltration was used to fractionate DOM, which has been demonstrated to be a promising fractionation method for DOM (Carlson et al. 1985; Guo et al. 1994; Guo and Santschi 1996). Water samples from Lake Biwa were chosen as a case study.

Materials and methods

Sampling

We selected two sampling stations in the north basin of Lake Biwa; Stations A (70m depth), and B (40 m depth), located in the northeast and southwest regions of the basin, respectively. Lake Biwa ($35^{\circ} 00' - 35^{\circ} 30' \text{ N}$, $135^{\circ} 50' - 136^{\circ} 15' \text{ E}$) is the largest freshwater source in Japan with a surface area of $674\ \text{km}^2$, a maximum depth of 104 m and a mean depth of 41 m. It is composed of two basins; the large, deep and mesotrophic North Basin and the small, shallow and eutrophic South Basin. Seasonal stratification usually occurs from April to January in Lake Biwa (Miyajima et al. 1997). Water samples were collected in June 1999, and were filtered through glass-fiber filters (GF/F, Whatman, Maidstone, UK) immediately after sampling, and stored at 2°C . The GF/F filtrate was then fractionated using a tangential flow ultrafiltration system (Minitan II system, Millipore Co. Ltd) with Durapore ($0.1\ \mu\text{m}$ pore size) and Biomax (cutoff membrane, molecular size 5 kDa) membranes successively. About 15 - 20 l of original water was concentrated to 200 - 400 ml in each fraction, namely, $0.1\ \mu\text{m}$ -GF/F and 5 kDa- $0.1\ \mu\text{m}$. The $<5\ \text{kDa}$ fraction was not concentrated. The fractionation was carried out within 2 days after GF/F filtration, and the fractions were then kept frozen until further analysis. The system was carefully pre-cleaned following the manufacturer's instructions.

All fractions were analyzed for DOC, fluorescence and absorbance. DOC concentration was measured by a high temperature catalytic oxidation method using potassium hydrogen phthalate as a standard; After the water sample was acidified with HNO_3 , and the DIC was removed by bubbling with pure air for 15 minutes, $200\ \mu\text{l}$ of sample was injected into TOC analyzer (TOC 5000A, Shimadzu Co. Ltd) (Wu et al. 2001). System and pure water (Milli-Q TOC, Millipore Co. Ltd) blanks were, on the average, $2 - 4\ \mu\text{MC}$ and $6\ \mu\text{MC}$, respectively.

Fluorescence was measured with 3DEEM using a fluorescence spectrophotometer (Hitachi, Model F-4500). The excitation wavelength ranged from 240 nm to 400 nm (5 nm bandwidth), and the emission from 250 nm to 600 nm (2 nm bandwidth). Each sample was scanned three times, and the resulting spectra were smoothed and averaged. The spectra were subsequently normalized to water Raman Scattering area, and MatlabTM was used to obtain the normalized 3DEEM surface and contour plots, in which Ex/Em maxima can be identified. Instrumental correction was made according to the manufacturer's instructions. UV absorbance of samples was measured at wavelength 254 nm using

a spectrophotometer (Shimadzu, MPS-2400, UV-vis multipurpose) equipped with a 2 cm quartz cell.

Amino acid analysis

Individual amino acid concentrations were determined by pre-column o-phthalaldehyde (OPA) derivatization and separation of the components by HPLC and fluorescence detection (Lindroth and Mopper 1979). For acid hydrolyzable amino acids, 2 ml water samples were hydrolyzed at 110°C for 22 h in 6N HCl. The hydrolysate was then diluted, neutralized with cooled 2N NaOH, and reacted with an OPA fluorescent tag for HPLC analysis. A reference mixture of 17 standard amino acids including aspartic acid (Asp), glutamic acid (Glu), serine (Ser), histidine (His), glycine (Gly), threonine (Thr), arginine (Arg), tyrosine (Tyr), alanine (Ala), methionine (Met), valine (Val), phenylalanine (Phe), isoleucine (Ile), leucine (Leu), ornithine (Orn), lysine (Lys) and proline (Pro) was used to assign the identities. Due to the nonlinear response, Orn, Lys and Pro were ignored. Since tryptophan (Trp) was not stable in the acid hydrolysis, alkaline hydrolysis was applied before HPLC analysis. For alkaline hydrolysis, ascorbic acid was added as antioxidant, and water samples were first hydrolyzed in 4.2N NaOH at 110°C for 16 h; The hydrolysate was then diluted, and neutralized to pH = 9 with cooled 2N HCl, reacted with a fluorescent tag and analyzed for tryptophan in a similar manner (Wu and Tanoue 2001b). The recovery of tryptophan was $91 \pm 3.3\%$ ($n = 4$). The analytical precision expressed as standard deviation from multiple standard injections of 25 μ l was less than 0.8% for Val, Met, Ile, Phe and Leu, 1.2–1.9% for Ser, His and Gly, 2.0–4.7% for Glu, Thr, Ala, Arg, Trp and Tyr, and 9.9% for Asp (Wu and Tanoue 2001b).

Results and discussion

Molecular size distribution of DOC, absorbance and fluorescence

The distribution of DOC, absorbance and fluorescence of the fractionated DOM is shown in Table 1. As determined by DOC concentration, the relative abundance of the <5 kDa fraction ranged from 55 to 69% of the total DOC, 5 kDa–0.1 μ m fraction from 30 to 43%, and 0.1 μ m–GF/F fraction from 1 to 2% (Table 1), indicating that most DOC was in the <5 kDa fraction. Relative DOC abundance in the <1 kDa fraction ranged from 50 to 78% in oceanic environments (Carlson et al. 1985; Guo et al. (1994, 1995); Guo and Santschi 1996). For freshwater, Martin et al. (1995) reported that only 43% of total DOC was in the <10 kDa fraction in Lena River. These results suggest that the relative abundance of DOC in the lower molecular size fractions varied among different environments. In terms of UV absorbance at 254 nm, the <5 kDa fraction accounted for 57–85% of the total DOM, which was slightly higher than those (55–69%) determined by DOC. For humiclike fluorescence, the <5 kDa molecular size fraction was also dominant, accounting for 74–88% of the total fluorescence. The recoveries for DOC, absorbance and fluorescence ranged from 84% to 121%, which are similar to the previous reports on DOC (80–118%, Carlson et al. (1985) and Guo et al. (1994, 1995), Guo and Santschi (1996)). Ultrafiltration systems that gave good fluorescence or absorbance balances may have poor DOC mass balances since fluorescence and absorbance techniques are more selective and thus may miss contaminants (Buesseler et al. 1996; Mopper et al. 1996). Good balances from all fluorescence, absorbance, DOC and THAA in this study indicate the validity of the ultrafiltration system used.

As seen in Table 1, Flu/Abs abundance ratios increased from 0.1 μ m–GF/F to 5 kDa–0.1 μ m, to the <5 kDa molecular size fraction, suggesting that the distribution was shifted towards the lower molecular fractions for humic-like fluorescence, as compared to UV absorbance. This is in agreement with previous reports that fluorescence efficiency or Flu/Abs ratios of DOM increased with reducing molecular weight (Stewart and Wetzel 1980; Ewald et al. 1988; Senesi 1990). The difference also implies that fluorescing and absorbing DOM was not evenly distributed over various molecular weights in freshwater.

3DEEM fluorescence characteristics of molecular size fractions

The normalized 3DEEM surface and contour plots of the fractionated DOM are shown in Figure 1. Two general Ex/Em maxima can be observed in these plots: Peak A with Ex/Em 320–350/430–460 nm, and Peak B with Ex/Em 230–250/430–470 nm. Part of the Peak B fluorescence was obscured by water Raman Scattering. Peaks A and B were similar to previous reports for DOM fluorescence in aquatic environments, and were usually referred to as humic-like fluorescence (Mopper and Schultz 1993; Coble 1996; Del Castillo et al. 1999; Wu et al. 2001).

It is interesting to note that an additional Peak C with Ex/Em 260–290/330–350 nm was obvious only in the

0.1 μm -GF/F fractions and GF/F filtrates. Fluorescence similar to Peak C in this study was also reported in

Table 1. Mass balances of DOC, absorbance, fluorescence and THAA of molecular size fractions of DOM in Lake Biwa.

Samples	Fractions	DOC $\mu\text{M C}^a$	Absorbance ^a at 254 nm(10^{-4} cm^{-1})	Fluorescence ^a Ex/Em 330/434 nm ^c	THAA ^d Concentration (nM) ^a	Ratios Flu/Abs ^e	THAA/DOC ^e
Station B							
2.5 m	GF/F filtrate	104	160	7.1	1106		(1.1)
	0.1 μm -GF/F	2 (2)	10 (7)	0.4 (5)	69 (7)	0.6 (0.04)	3.5 (3.3)
	5 kDa-0.1 μm	40 (43)	50 (36)	1.8 (21)	411 (42)	0.6 (0.04)	1.0 (1.0)
	< 5 kDa	51 (55)	80 (57)	6.4 (74)	500 (51)	1.3 (0.08)	0.9 (1.0)
	Sum of 3 fractions	93 (100)	140 (100)	8.6 (100)	980 (100)		
	Recovery (%) ^b	89	88	121	89		
	70 m	GF/F filtrate	89	132	8.4	975	
0.1 μm -GF/F	1.0 (1)	4 (3)	0.2 (2)	83 (8)	0.6 (0.05)	8.0 (8.0)	
5 kDa-0.1 μm	28 (30)	18 (12)	1.0 (10)	302 (29)	0.8 (0.06)	1.0 (1.1)	
< 5 kDa	65 (69)	125 (85)	8.4 (88)	655 (63)	1.0 (0.07)	0.9 (1.0)	
Sum of 3 fractions	94 (100)	147 (100)	9.6 (100)	1042 (100)			
Recovery (%) ^b	106	111	114	107			
Station A							
2.5 m	GF/F filtrate	107	190	9.8	1530		(1.4)
	0.1 μm -GF/F	2 (2)	10 (6)	0.5 (5)	156 (11)	0.8 (0.05)	5.5 (7.8)
	5 kDa-0.1 μm	47 (40)	30 (19)	1.9 (18)	540 (38)	0.9 (0.06)	1.0 (1.1)
	< 5 kDa	67 (58)	120 (75)	8.1 (77)	724 (51)	1.0 (0.07)	0.9 (1.1)
	Sum of 3 fractions	116(100)	160 (100)	10.5 (100)	1420 (100)		
	Recovery (%) ^b	108	84	107	93		

^aThe value was estimated as that in the original water. The value in the parentheses denoted that of each fraction as a percentage of the sum for all fractions. ^bRecovery was expressed as a proportion of the sum of all fractions relative to the value for the GF/F filtrate. ^cThe unit was arbitrary. ^dTHAA denoted total hydrolyzed amino acids. ^eRatios were based on their relative abundance, and the values in the parentheses were based on their contribution.

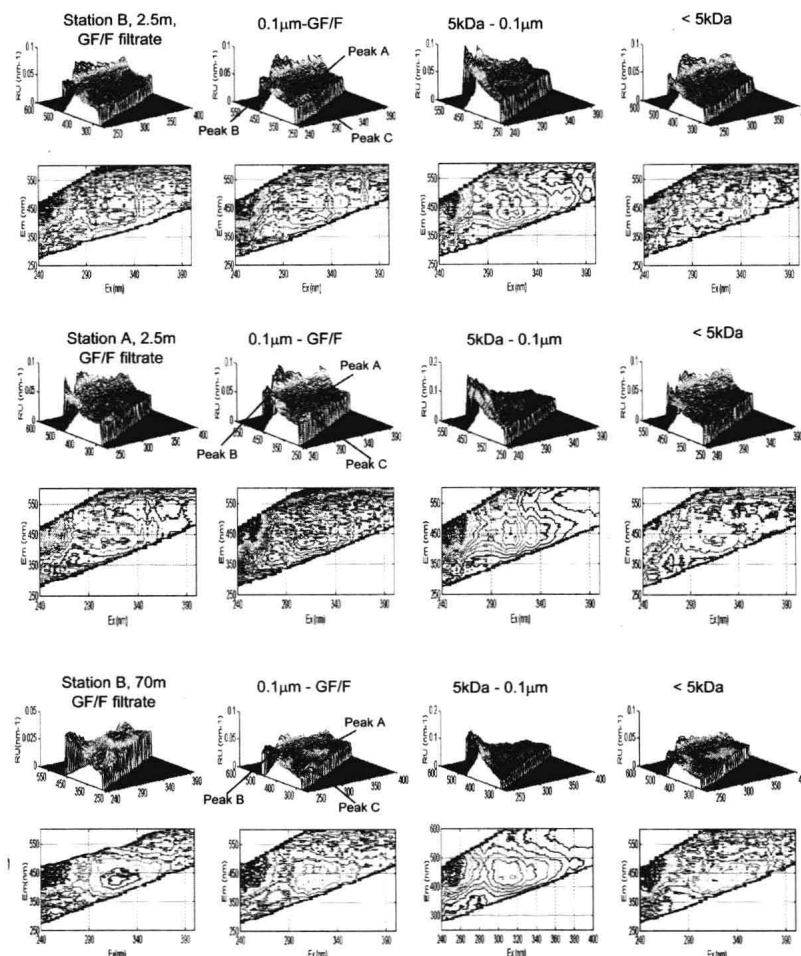


Figure 1. 3DEEM surface and contour plots of molecular size fractions of DOM in Lake Biwa. The fluorescence was calibrated by water Raman scattering. The fractions were the same as those in Table 1.

other natural waters (280/325 – 335 nm, Coble et al. (1990); 270/320 nm, Mopper and Schultz (1993); 270/320 nm, Determann et al. (1994) and Wu et al. (2001)), and was usually referred to as protein-like fluorescence. Determann et al. (1994, 1998) reported that some phytoplankton, picoplankton and bacteria were the major sources of protein-like fluorescence in natural aquatic environments. Our results are consistent with those reports since the 0.1 μm -GF/F fraction may possibly include small phytoplankton and bacteria particles.

Thus, differences in fluorescence properties were evident for different molecular size fractions of DOM. The humic-like and protein-like fluorescence was shifted to the lower and higher molecular size fractions, respectively.

Amino acids in various molecular size fractions, and their relationship with fluorescence characteristics

Total hydrolyzed amino acids (THAA) included total acid hydrolyzed amino acids and alkaline hydrolyzed tryptophan. THAA concentrations and composition in various molecular size fractions of DOM are shown in Tables 1 and 2. The mass balance ranged 89 – 107%, and was again satisfactory. The <5 kDa molecular size fraction accounted for 51 – 63% of total THAA, indicating that major THAA were in the <5 kDa fraction. This result is similar to fluorescence and absorbance distribution discussed earlier. However, THAA/DOC ratios increased with increasing molecular size (Table 1), showing that THAA were more heavily weighted in the higher molecular size fractions than in the lower molecular fractions.

Molar percent ratios of individual amino acids in THAA in different molecular size fractions were analyzed to identify differences in composition (Figure 2, Table 2). It is shown that the most abundant species were Ala, Asp, Glu, Gly and Ser in all molecular size fractions, accounting for 53.4–58.4% of total THAA.

Amino acids in different molecular size fractions have not been well documented in aquatic environments. At present, only a few studies have been done in freshwaters, and these have mainly focused on comparison between particulate and dissolved fractions (Mayers et al. 1984; Coffin 1989; Berdie et al. 1995). Amino acids have been extensively studied in bulk DOM, sediments and particulate in aquatic environments (Siezen and Mague 1978; Lee and Cronin 1984; Steinberg et al. 1987; Burdige and Martens 1988; Colombo et al. 1998; Dauwe and Middelburg 1998). These previous studies demonstrated that despite overall similarity of amino acid composition in sediments, particulate and setting particle in the water column, evident differences (composition and concentration) with depth existed, indicating organic matter degradation. It was also reported that glutamic acid, aromatic tyrosine and phenylalanine were labile, while glycine, serine and threonine were selectively preserved in degradation.

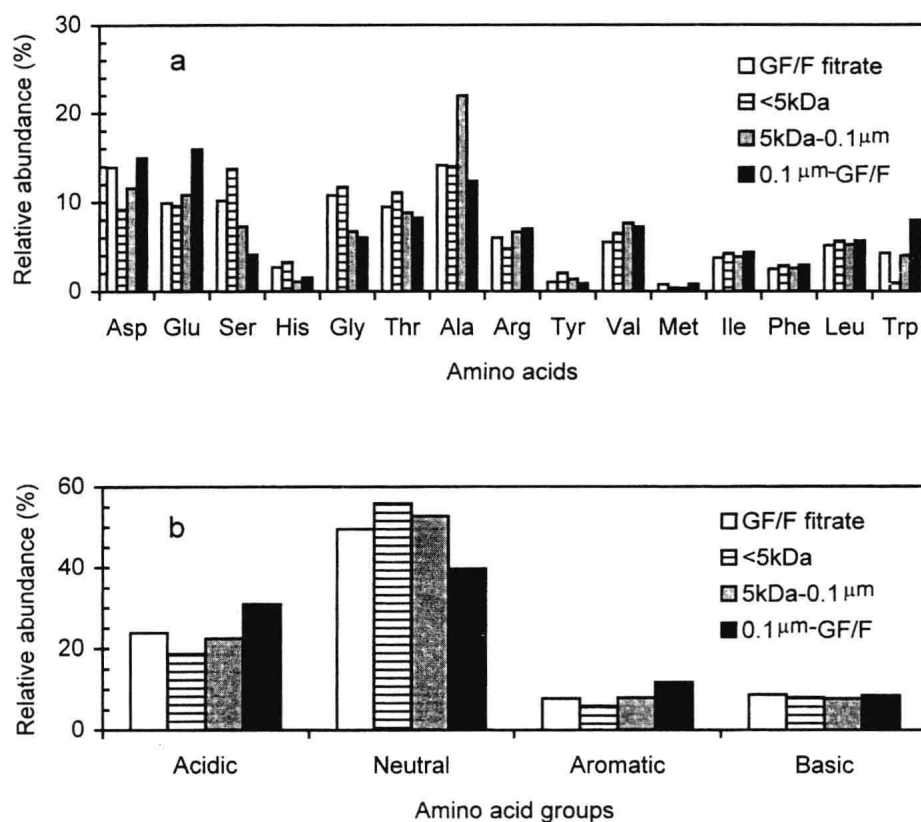


Figure 2. The average relative abundances of amino acids and their functional groups in molecular size fractions of DOM in Lake Biwa.

Our data (Table 2 and Figure 2a) show that the relative abundance of aspartic acid and glutamic acid decreased with reducing molecular size (from 0.1 μm-GF/F, to 5 kDa-0.1 μm, to the <5 kDa fractions), while that of glycine and serine increased. This finding may imply that amino acids were good biomarkers for DOM degradation, possibly tracing the occurrence of organic matter degradation from higher to lower molecular weight. This is strongly supported by the higher nitrogen abundance and lability of higher molecular size fractions of DOM in recent studies (Hollibaugh and Azam 1983; Harvey et al. 1995), and is also consistent with the fact that THAA contribution to total DOC decreased from the higher to lower molecular size fractions (Table 1), as this may suggest the preferential removal of THAA relative to organic carbon during degradation. The fluorescence results discussed in earlier sections also support our suggestion since the <0.1 μm fractions were dominated by humic-like fluorescence, which was reportedly resulted from refractory organic materials (Mopper and Schultz 1993; Determann et al. 1994); only the 0.1 μm-GF/F fraction had the protein-like fluorescence, which was linked to recent biological origin (e.g. Traganza (1969) and Mopper and Schultz (1993)). Moran et al. (2000) observed that protein-like fluorescence was increased during DOM biological degradation experiments, suggesting that biological degradation would not be possibly responsible for the DOM degradation from higher to lower molecular weight. Photochemical degradation may be the most likely process as this has been widely reported to play key roles in controlling the degradation of DOM in aquatic environments (e.g. Zepp (1998) and Moran et al. (2000)).